Research article

Development and thermo-mechanical behavior of nanocomposite epoxy adhesives

Andrea Dorigato[a]* and Alessandro Pegoretti[a]

Two kinds of organo-modified (OM) clays were dispersed in an epoxy resin for the preparation of nanocomposite adhesives at various filler amounts. XRD tests evidenced the formation of intercalated structures, increasing the intercalation degree with the clay hydrophilicity. The original transparency of the samples was retained up to a filler content of 3 wt%, and then decreased due to filler agglomeration. The glass transition temperature of nanocomposites filled with the more hydrophilic clay (30B) raised up to a filler content of 3 wt% and then decreased, probably because of the concurrent and contrasting effects of the physical chain blocking and reduction of the cross-linking degree. Also elastic modulus, stress at break, and fracture toughness were sensibly improved by nanoclay addition up to filler loadings of 0.5–1 wt%. For higher concentrations the positive contribution of clay nanoplatelets was counterbalanced by the presence of agglomerated tactoids in the matrix. Mechanical tests on single-lap composite (epoxy/glass) bonded joints evidenced an enhancement of the shear strength by about 25% for an optimal filler content of 1 wt%. Therefore, it was concluded that the addition of a proper amount of OM clay to epoxy adhesives could represent an effective way to improve the shear resistance of adhesively bonded composite structures. Copyright © 2011 John Wiley & Sons, Ltd.

Keywords: adhesives; clay; nanocomposites; bonded joints

INTRODUCTION

The use of adhesives in place of traditional fasteners is becoming increasingly popular in structural design, because of their reduced weight and cost. A comprehensive review of the advances in bonding with structural adhesives has been recently edited by Dillard.[1]

In the last years, epoxy resins reached a preeminent position among structural adhesives, as they are widely utilized in aerospace, automotive, electronic, domestic household, oil, and other industries.[2] A heavy drawback that limited an extensive development of epoxy resins as structural adhesives for joining polymer composite components is represented by their inherent brittleness, and several investigations were thus performed to increase the fracture toughness of these systems. In particular, it was demonstrated that the crack resistance of structural epoxy adhesives could be improved by the incorporation of elastomeric micro- or nanodomains.[2–4] As an example, He et al.[5] analyzed the fracture behavior of rubber modified epoxy systems, showing that the toughness was increased up to an optimal rubber content. On the other hand, the addition of rubber to a glassy epoxy network is often detrimental for the rigidity and long-term (creep) mechanical properties of the adhesive.[6] Another possibility is offered by the incorporation of rigid nanofillers[7,8] into the epoxy matrix. In fact it was recently demonstrated that the addition of small quantities of inorganic nanoparticles in polymeric adhesives can improve the shear resistance of structural joints.[9] The enhancement of the mechanical performances of the epoxy adhesives can be directly related to the improved shear strength of nanomodified joints.[10] Moreover, the presence of small amounts of nanofiller may also improve the wetting capability of the epoxy matrix itself, thus improving their adhesion to the substrate.[11,12] In addition, it has been reported that, due to their small dimensions, nanofillers could penetrate into any small void on the adherend surface, thus enhancing the joint strength by mechanical interlocking.[13] In other cases, it was observed that the failure mechanism completely changes due to presence of nanoparticles in the adhesive.[14,15] As an example, Patel et al.[16] synthesized nanocomposite adhesives by solution polymerization of acrylic polymers in presence of nanosilica or clay, and investigated the adhesion behavior of the hybrid adhesives against different substrates (aluminum, wood, and polypropylene). In the case of aluminum and wood, the bonded joints displayed an higher shear strength attributed to the interaction of the adhesive with the hydroxyl groups of the substrates surface. Park and Lee[17] utilized carbon black nanoparticles in order to improve the mechanical performances and the durability of composite (glass/epoxy) adhesively bonded joints. The lap shear strength and the durability under thermal loadings was significantly enhanced, because of the better thermal stability and lower thermal expansion coefficient of carbon black reinforced adhesive. Xi et al.[18] analyzed the electrical conductivity and the shear strength of electroconductive adhesives, prepared from polyurethane resins filled with different kind of modified graphites. They found that the strength of the adhesive joints on aluminum increased up to a filler content of 20 wt%. Yu et al.[19] developed epoxy adhesives reinforced with carbon nanotubes (CNTs), to be utilized in aluminum joints, concluding that the addition of CNTs in

* Correspondence to: A. Dorigato, Department of Materials Engineering and Industrial Technologies, University of Trento, via Mesiano 77, 38123 Trento, Italy.
E-mail: andrea.dorigato@ing.unitn.it

a A. Dorigato, A. Pegoretti
Department of Materials Engineering and Industrial Technologies, University of Trento, via Mesiano 77, 38123 Trento, Italy

Copyright © 2011 John Wiley & Sons, Ltd.

concentrations up to 1 wt% greatly improved the durability of epoxy-based adhesive joint in tests under water at 60°C.

For as concerns epoxy-based nanocomposites, several papers can be found on the addition of metal oxides, mainly silica[20–22] and zirconia[23,24] nanoparticles. However, the major part of available literature in this field is focused on the preparation and characterization of layered silicates (clays) filled systems.[22,25–33] The thermo-mechanical behavior of polymer–clay nanocomposites is strongly dependent on the dispersion level of the clay nanoplatelets in the polymer matrix, which in turns is influenced by the filler–matrix interactions.[34,35] Basara et al.[27] studied the effects of the clay content and typology on mechanical properties of epoxy/clay nanocomposites, finding that the tensile modulus, the tensile strength, and the impact strength were strongly improved by nanofiller addition. Liu et al.[36] synthesized epoxy/clay nanocomposites through a solution dispersion technique and observed interesting improvements of the fracture toughness, accompanied by a significant reduction in the water diffusivity and water uptake. Zunjarrao et al.[37] investigated the influence of processing parameters and particle volume fraction of epoxy/clay nanocomposite systems, prepared through high-speed shear dispersion and ultrasonic disruption techniques, concluding that both the flexural modulus and the fracture toughness increased at low clay volume fractions. Moreover, it has been recently observed that also the fiber–matrix adhesion[38] can be improved by the addition of organo-modified (OM) clays in the matrix of glass/epoxy composites.[39]

Starting from these considerations, in the present study we focused our attention on the effect of two different kind of OM clays on the thermal and mechanical behavior of an epoxy adhesive, to be then utilized for the preparation of composite (glass/epoxy) adhesively bonded joints.

EXPERIMENTAL PART
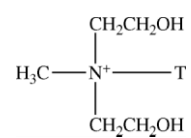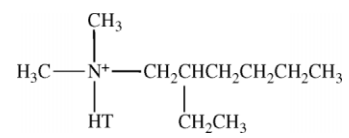
Bulk adhesives preparation and characterization

A two components epoxy resin suitable for the preparation of commercial adhesives was supplied by Elantas® Camattini (Collecchio, Italy). An EC57 epoxy base (density and viscosity at 25°C of 1.15 g cm^{-3} and 1500 mPa s, respectively), constituted by a mixture of di-glycidyl ether of bisphenol A (75–100%),

hexanediol diglycidyl ether (10–20%), and di-glycidyl ether of bisphenol F (10–20%), was mixed at a weight ratio of 100:50 with a W635 hardener (density and viscosity at 25°C of 0.95 g cm^{-3} and 750 mPa s, respectively), constituted by a mixture of polyaminoamides. Two different OM clays (Cloisite® 30B and Cloisite® 25A), provided by Southern Clay Products, Inc. (Gonzales, Texas) were used. In a previous investigation of this research group,[35] water–clay equilibrium contact angle measurements were successfully adopted to rank several OM clays accordingly to their hydrophobicity. In particular, it was proven that Cloisite® 25A was more hydrophobic than Cloisite® 30B. Table 1 summarizes some of the physical characteristics of the selected OM clays.

Various filler contents (from 0.5 to 5 wt%) were added to the epoxy base and mechanically mixed for 1 hr in a Dispermat® F1 high-shear mixer operating at 2000 rpm. An ultrasonication treatment was then performed through an Hielscher UP400S sonicator for 5 min at a specific power of 460 W cm^{-2} and a frequency of 24 kHz. The mixture was then degassed at ambient temperature and the amine hardener added and manually mixed for 5 min. Finally, the mixture was degassed again at ambient temperature and poured in the cavities of a silicone mould. A curing cycle at 65°C for 15 hr was then conducted. The same procedure was followed also for the preparation of unfilled adhesive. The samples were denoted indicating the matrix (Epoxy), the kind of clay (30B or 25A), followed by the filler weight fraction. For instance, the adhesive filled with 1 wt% of Cloisite 25A was indicated as Epoxy-25A-1.

Samples of neat epoxy and of the relative nanocomposites were cryofractured in liquid nitrogen and metalized before observations by a Zeiss Supra 40 field emission scanning electronic microscope (FESEM), at an acceleration voltage of 2 kV and a pressure of 10^{-6} Torr (magnification of 5000×). X-ray diffraction (XRD) analysis was conducted on fully cured bulky samples, in order to evaluate the dispersion level of the clay nanoplatelets in the adhesive. A Philips XPert MRD diffractometer, operating at a voltage of 40 kV and a current of 45 mA, with a non-monochromatized copper radiation of 0.15406 nm wavelength, was utilized. The interlayer distance (d_{001} spacing) of pristine clays and of the same dispersed in the epoxy matrix was evaluated. An intercalation degree (ID), representing the increase of the d_{001} spacing with respect to the original value, was determined as previously described.[35]

Table 1. Organo-modified clays utilized in the present work					
Trade name	Organic modifier (OM)	OM concentration [meq/100 g clay]	Density [g cm^{-3}]	d_{001} spacing [nm]	VIECA (°)
Cloisite 30B	H₃C—N⁺—T with CH₂CH₂OH and CH₂CH₂OH	90	1.87	1.85	23.1 ± 0.1
Cloisite 25A	H₃C—N⁺—CH₂CHCH₂CH₂CH₂CH₃ with CH₃, HT and CH₂CH₃	95	1.87	1.86	50.9 ± 1.9
VIECA, vibration induced equilibrium contact angle with water; T, Tallow (∼65% C18; ∼30% C16; ∼5% C14); HT, Hydrogenated Tallow.					

The optical transparency of 2 mm thick adhesive samples was evaluated using a Nikon Coolpix 4500 digital camera at a distance of 30 cm. Environmental scanning electron microscopy (ESEM) observations were performed with a Philips XL30 microscope, operating at an acceleration voltage of 30 kV and a pressure of 0.6 Torr. ESEM observations were collected on the fracture surfaces of specimens broken for fracture toughness tests (see below).

Differential scanning calorimetry (DSC) analysis was performed by a Mettler DSC30 apparatus. A thermal ramp, from 0 to 220°C at a heating rate of 10°C min^{-1}, under a nitrogen flow of 100 ml min^{-1}, was applied.

Quasi-static tensile properties of bulk adhesives were evaluated by using an Instron 4502 electromechanical testing machine. ISO-527 1BA dogbone specimens, with a gage length of 30 mm, a width of 5 mm, and a thickness of 2 mm, were tested at a crosshead speed of 0.25 mm min^{-1}. The axial deformation was monitored through an Instron 2620-601 clip-on extensometer, having a gage length of 12.5 mm. Following ISO 527 standard, the elastic modulus was calculated as a secant value between the strain levels of 0.05% and 0.25%. All tests were conducted at ambient temperature (23°C), and at least five specimens were tested for each sample. According to ASTM D5045 standard, plane strain fracture toughness parameters K_{IC} and G_{IC} were evaluated on single edge notched bend (SENB) specimens (44 mm long, 10 mm wide, and 4 mm thick) containing a sharp notch 5 mm deep. A crosshead speed of 10 mm min^{-1} was adopted under three point bending configuration, and at least five specimens were tested for each sample.

Single-lap bonded joints preparation and characterization

Square sheets of epoxy–glass composite laminates, having a width of 300 mm and a thickness of 2.3 mm, were prepared by hand lay up with a [0/90/−45/+45/+45/−45/90/0] lamination sequence. A bi-component epoxy resin for manual lamination, supplied by Elantas® Camattini, was utilized in combination with glass fibers fabrics for the preparation of composite laminates to be utilized as adherends of the single lap joints. An EC152 epoxy base (density at 25°C of 1.15 g cm^{-3}) was mixed with a W152 LR hardener (density at 25°C of 0.92 g cm^{-3}) at a weight ratio of 100:30. Epoxy compatible sized glass fiber woven fabrics, having a specific weight of 400 g m^{-2}, were provided by Schaller (Florence, Italy). After a preliminary degassing in a vacuum bag, the laminates were cured in a Carver® laboratory press at 50°C for 2 hr followed by 80°C for 2 hr. According to ASTM D 1002 standard, rectangular adherends were machined with a length of 101.6 mm and a width of 25.4 mm. The epoxy adhesive used for the preparation of single-lap bonded joints was the same utilized for bulk adhesives samples (i.e. the system EC57/W635 with or without filler). The adherends were sand-papered and washed in acetone and the epoxy adhesive was then carefully poured over an overlapping area of 25.4 × 12.7 mm^2. The thickness of the adhesive layer was fixed at 0.5 mm by a proper PTFE mask. The joints were then cured under the same conditions adopted for the bulk adhesives (i.e. at 65°C for 15 hr).

The bonded joints were mechanically tested at ambient temperature (23°C) under quasi-static loading conditions by using an Instron 4502 electromechanical tensile testing machine. According to ASTM D1002 standard, a crosshead speed of 1.3 mm min^{-1} was adopted. At least five specimens were tested

for each sample. A nominal shear strength was computed as:

$$\tau_{max} = \frac{F_{max}}{A} \tag{1}$$

where F_{max} is the maximum load registered during the tensile tests and A is the overlapping area of the joint.

RESULTS AND DISCUSSION

Bulk adhesives

In order to collect information about the dispersion of the clay nanoplatelets in the epoxy matrix, FESEM was utilized. In Fig. 1 FESEM micrographs of the fracture surfaces of pure Epoxy and relative nanocomposites are reported. As expected, the surface of the pure epoxy sample is very smooth (Fig. 1a), while at low filler contents (0.5 wt%) only small aggregates with submicron dimension, constituted by the stacking of clay nanoplatelets, can be observed (Fig. 1b,e). Increasing the filler content at 1 wt%, it is evident the presence of clay tactoids with irregular shape and random orientation in the matrix, having a mean size of 2–3 μm (Fig. 1c,f). It is interesting to note that the mean size of the aggregates of 25A clay nanofilled samples is slightly higher than that of 30B nanocomposites, probably indicating that a better dispersion was achieved by using more hydrophilic clay. Increasing the clay loading up to 5 wt%, further agglomeration of the clay lamellae occurs (Fig. 1d,g). The presence of clay tactoids probably suggests that at high filler contents the complete exfoliation of clay nanoplatelets was not achieved, and that an intercalated structure could be obtained for these samples. A similar aggregated morphology was already observed by Liu et al.[36] on epoxy/clay nanocomposite samples prepared by a solution dispersion technique, and by Nigam et al.[40], which investigated the morphological and thermal behavior of epoxy/montmorillonite systems prepared by swelling different proportions of the clay in a diglycidyl ether of bisphenol-A (DGEBA), followed by in situ polymerization with aromatic diamine. It is clear that the presence of nanoclay clusters in the epoxy matrix at elevated clay loadings could play an important role on the mechanical behavior of nanofilled adhesives.

XRD patterns of the prepared nanocomposite adhesives are compared in Fig. 2, while the most relevant parameters are summarized in Table 2. Pristine Cloisite 30B clay presents a well-defined diffraction peak at $2\theta = 4.8°$, corresponding to an interlamellar spacing of 1.83 nm. In the case of both Epoxy-30B-3 and Epoxy-30B-5 bulk adhesives, a shift of the diffraction peak to lower angles (about 2.3°) can be observed. An increase of the interlamellar spacing with respect of the original clay powders suggests that these nanocomposites are characterized by an intercalated structure. Interestingly, no diffraction peaks can be detected for samples containing a lower amount of Cloisite 30B clay, and an exfoliated structure can be hypothesized. Even if from Fig. 1c clay tactoids having a mean width of 2–3 μm were observed, it is probable that in Epoxy-30B-1 sample the major part of the clay lamellae are in a completely exfoliated state, or that the interlamellar spacing between clay nanoplatelets is too high to be detected in the diffraction pattern of this sample. It is interesting to note how Epoxy-30B-3 and Epoxy-30B-5 samples present a relatively weak and broad diffraction signal at 2θ around 4°, which corresponds to an interlamellar spacing of about 21 nm. It can be hypothesized that these reflections
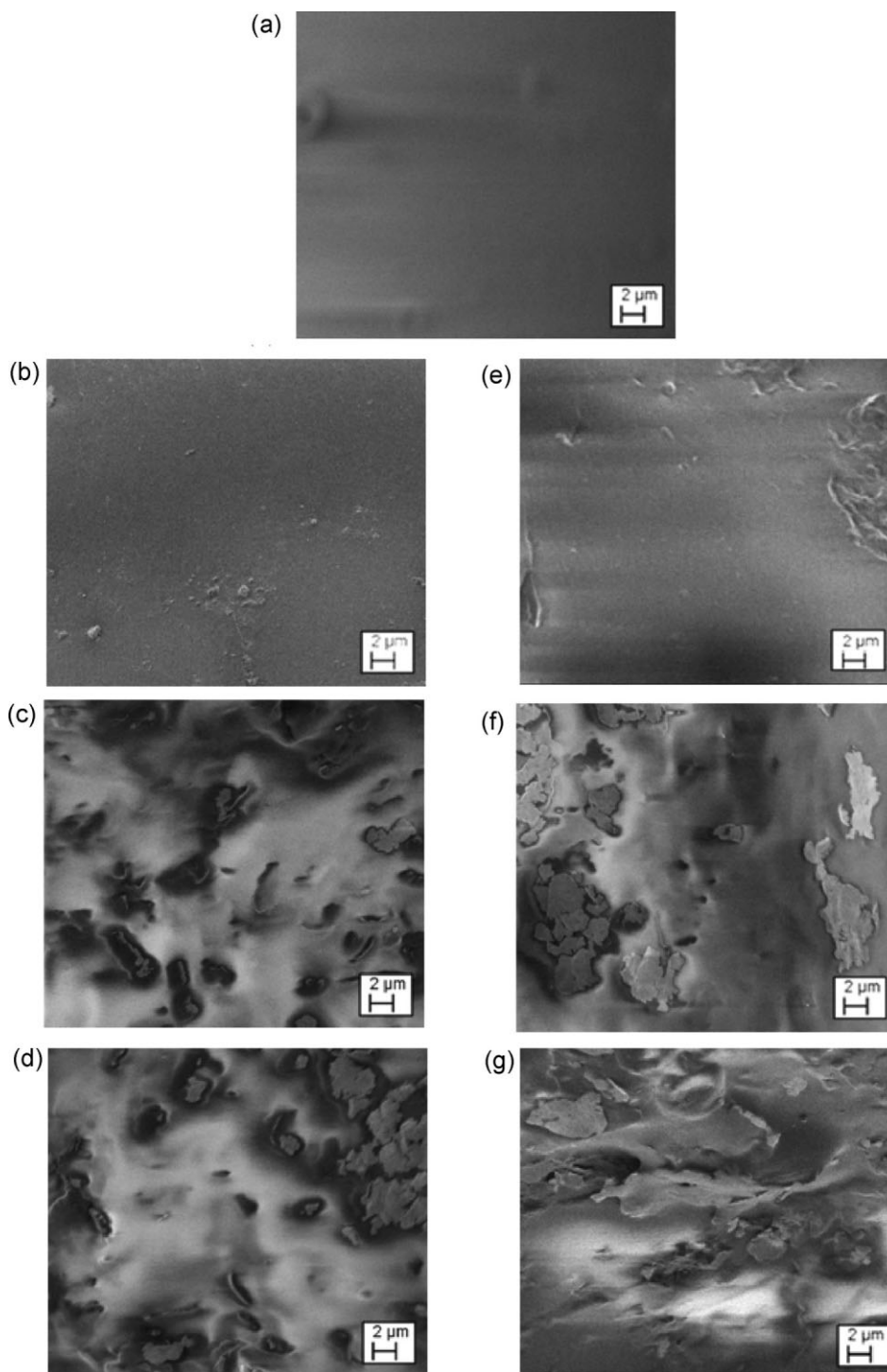
Figure 1. FESEM images of the fracture surfaces of pure Epoxy and relative nanocomposites. (a) Epoxy, (b) Epoxy-30B-0.5, (c) Epoxy-30B-1, (d) Epoxy-30B-5, (e) Epoxy-25A-0.5, (f) Epoxy-25A-1, and (g) Epoxy-25A-5.

are due to the presence of a fraction of clay tactoids at lower ID within the matrix. Even if a complete exfoliation of the clay lamellae is sometimes reported,[41] the formation of an intercalated structure is more commonly documented in the existing literature on epoxy–clay nanocomposites.[25,27,28,36,37,42] Similar conclusions can be drawn for Cloisite 25A filled composites, with an increase of the interlamellar spacing from $2\theta = 4.2°$ to $2\theta = 2.5°$ for 3 and 5 wt% nanocomposites and the
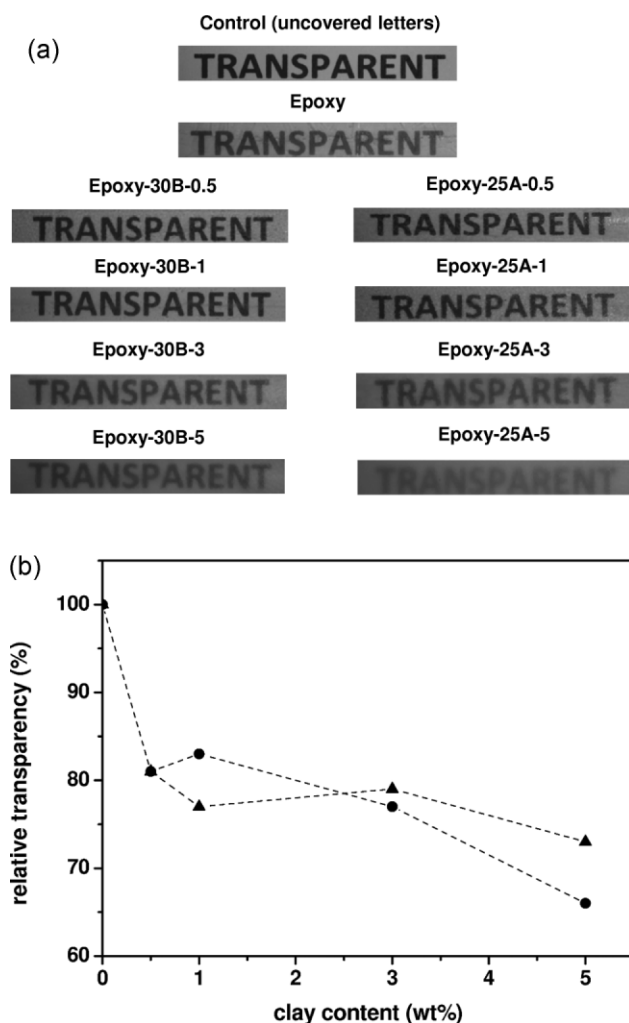
disappearance of the diffraction peak at lower clay loadings. It is important to note that the ID is higher for the most hydrophilic clay (30B). This means that epoxy–clay interactions and the consequent dispersion of the clay nanoplatelets improve as the clay hydrophilicity increases. Similar results were reported by this research group in a previous investigation on poly-urethane–clay nanocomposites.[35] The outlined differences in the interfacial interaction and clay dispersion in the epoxy matrix
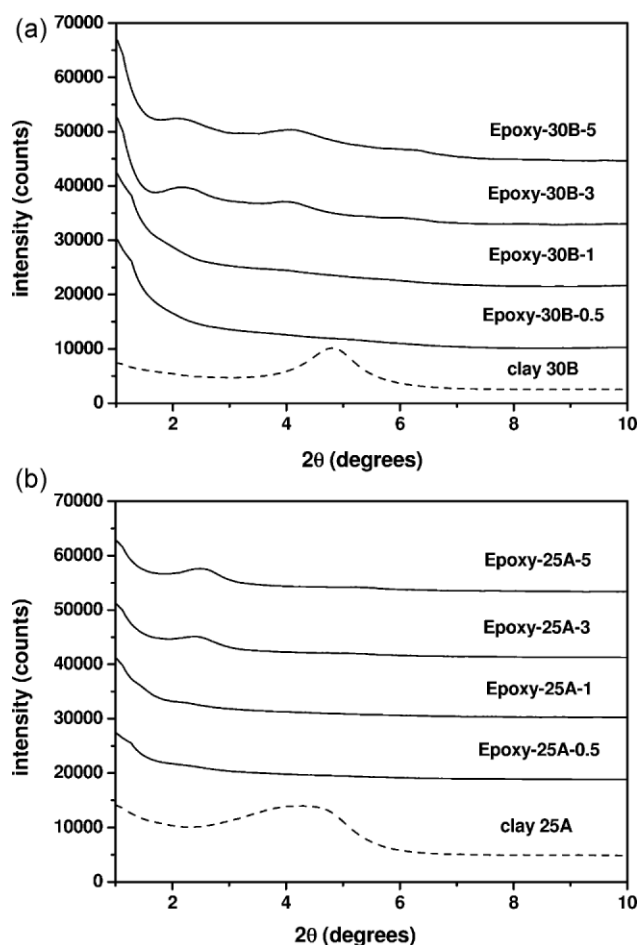
Figure 2. XRD patterns of epoxy–clay bulk adhesives filled with various amounts of (a) Cloisite 30B, and (b) Cloisite 25A clays.

could play an important role on the thermo-mechanical response of the filled adhesives.

The optical transparency of the nanofilled bulk adhesives is compared in Fig. 3a with that of the neat epoxy resin. The relative transparency values reported in Fig. 3b have been evaluated as the ratio between the pixels intensity on a gray scale of the printed letters located behind the specimens and that of the same uncovered letters (control in Fig. 3a). It can be noticed that

Table 2. Interlayer distance (d_{001} spacing) and intercalation degree (ID) of epoxy–clay bulk adhesives

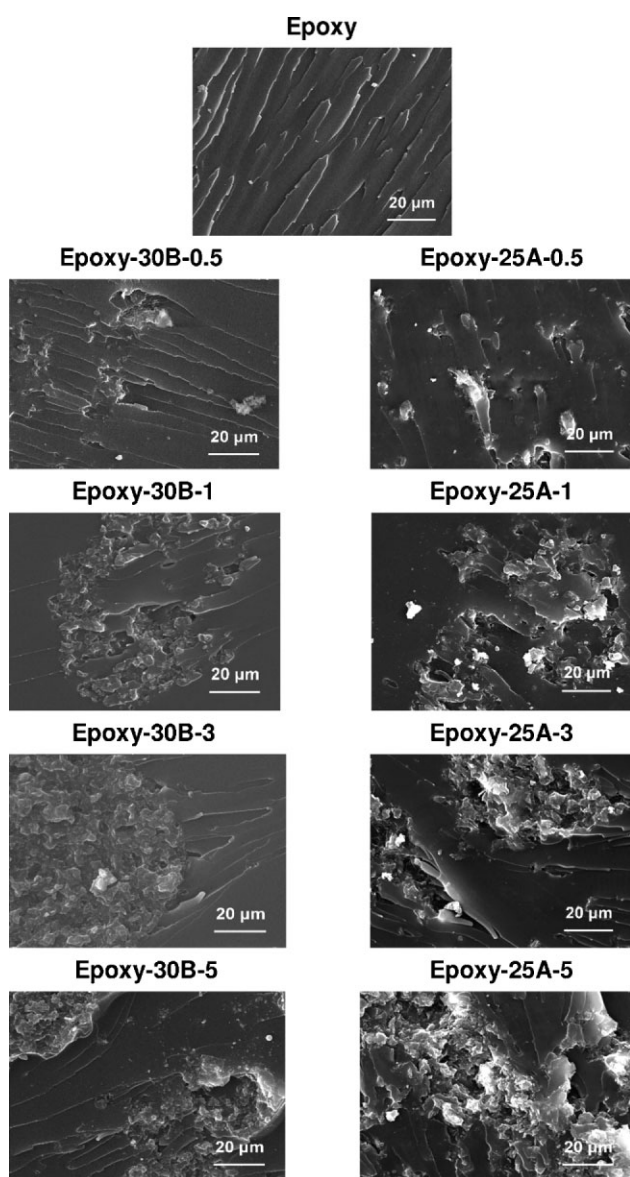| Sample	d_{001} (nm)	ID (%)
30B clay	1.83	—
Epoxy-30B-0.5	Not detectable	—
Epoxy-30B-1	Not detectable	—
Epoxy-30B-3	3.98	117.5
Epoxy-30B-5	4.17	127.9
25A clay	2.10	—
Epoxy-25A-0.5	Not detectable	—
Epoxy-25A-1	Not detectable	—
Epoxy-25A-3	3.65	73.8
Epoxy-25A-5	3.50	66.7

Figure 3. (a) Photographs for the evaluation of the optical transparency and (b) relative transparency values of epoxy–clay bulk adhesives filled with various amounts of (▲) Cloisite 30B, and (●) Cloisite 25A clays.

nanocomposites retain most of their original transparency up to a filler content of 3 wt%, and only at higher clay concentrations their optical clarity is slightly impaired. Even if FESEM images in Fig. 1 reveal the presence of aggregated clusters at elevated clay loadings, the transparency of the nanofilled samples means that a relatively good dispersion of the clay nanoplatelets is achieved during the mixing process even at high filler amounts. Furthermore, transparency of bulk adhesive filled with 5 wt% of Cloisite 30B is slightly higher than that of Cloisite 25A filled samples, thus confirming the better dispersion levels evidenced in XRD tests for the more hydrophilic clay.

ESEM observations of the fracture surfaces of pure epoxy adhesive and relative nanocomposites are collected in Fig. 4. It can be noticed that the morphology of the fracture surfaces is strongly affected by the presence of the OM clays. In fact, while the appearance of the fracture surface of pure epoxy resin is relatively smooth, more corrugated surfaces can be observed for nanofilled samples. Interestingly, surface corrugation appears to be more and more intense as the filler content increases. The corrugation of the fracture surfaces induced by the presence of OM clay dispersed in epoxy resins is well documented in the scientific literature,[25,36,43] and the creation of a higher amount of fracture surface is often correlated to a toughening effect.
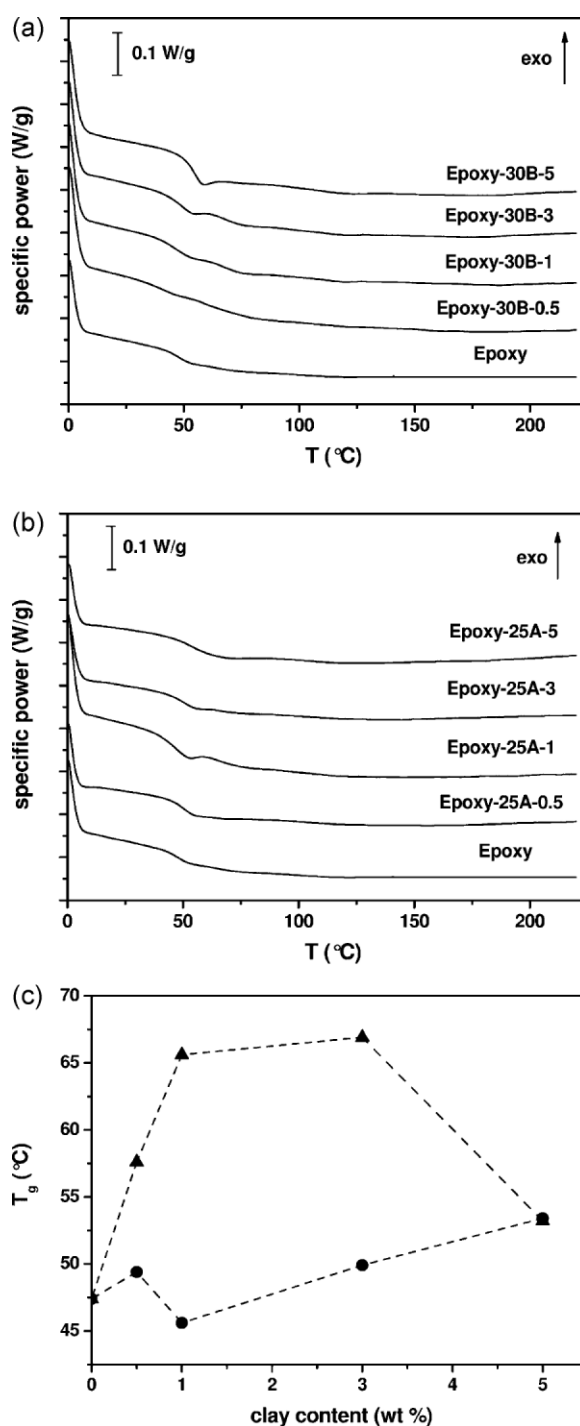
Figure 4. ESEM images of the fracture surfaces of pure epoxy adhesive and relative nanocomposites.

Figure 5. Representative DSC tests on epoxy–clay bulk adhesives filled with various amounts of (a) Cloisite 30B and (b) Cloisite 25A clays. (c) Glass transition temperatures (T_g).

Considering the DSC thermograms reported in Fig. 5 it results that all samples are fully cured. Moreover, as represented in Fig. 5c, the glass transition temperature (T_g) increases due to the introduction of the OM clay, thus confirming the observations reported by Dean et al.[28] on the chemorheological behavior of epoxy-layered silicate nanocomposites. In the case of nanocomposites filled with Cloisite 30B, a maximum T_g increment occurs for a filler loading of 3 wt%, while for higher clay contents the glass transition temperature starts to decrease. As previously reported for polyurethane–clay nanocomposites,[35] the occurrence of two concurrent and opposite phenomena could be invoked to explain the observed trend of T_g values. In fact, as the filler content increases, a chain blocking effect due to polymer–filler interaction is likely to occur and, at the same time, polymer–filler chemical interactions at a nanoscale could hinder the cross-linking process of the matrix.[20] On the other hand, nanocomposites filled with Cloisite 25A show only a slight enhancement of the T_g with the filler content. It could be

hypothesized that the lower degree of interfacial interaction may led to a weak chain blocking mechanism and negligible effects on the cross-linking degree of the resin.

Table 3 summarizes the most important parameters detected from the stress–strain curves of epoxy–clay nanocomposites measured under quasi-static tensile tests (curves not reported for the sake of brevity). For both clays types, the elastic modulus (E) slightly increases up to a clay concentration of 1 wt% (+32% with respect to the pure matrix), and then starts to decrease for

Table 3. Quasi-static tensile mechanical properties of epoxy–clay bulk adhesives

Sample	E (GPa)	σ_b (MPa)	ε_b (%)
Epoxy	2.29 ± 0.07	35.9 ± 1.3	5.1 ± 0.9
Epoxy-30B-0.5	2.90 ± 0.09	43.0 ± 1.2	4.9 ± 0.2
Epoxy-30B-1	3.04 ± 0.07	43.1 ± 1.1	5.0 ± 0.3
Epoxy-30B-3	2.65 ± 0.04	36.1 ± 0.9	2.6 ± 0.2
Epoxy-30B-5	2.41 ± 0.09	35.7 ± 0.9	3.6 ± 0.2
Epoxy-25A-0.5	3.00 ± 0.10	45.3 ± 1.3	3.8 ± 0.6
Epoxy-25A-1	2.99 ± 0.08	40.0 ± 1.6	3.5 ± 0.3
Epoxy-25A-3	2.58 ± 0.04	37.2 ± 0.9	2.1 ± 0.2
Epoxy-25A-5	2.47 ± 0.09	31.6 ± 1.0	2.1 ± 0.2

higher clay loadings. Interestingly enough, the introduction of clay leads to an improvement of the tensile strength (σ_b) with respect to the neat resin up to an optimal filler loading (0.5–1 wt%). On the other hand, strain at break values (ε_b) gradually decrease as the clay content increases, especially in the case of Cloisite 25A filled samples. According to the existing literature indications,[25,29,31] the slight drop of the quasi-static tensile properties experienced at elevated filler amounts could be attributed to the presence of a fraction of non-intercalated clay tactoids with micrometric dimension acting as crack nucleation sites. Therefore, the reinforcing effect due to the dispersion of clay nanoplatelets is counterbalanced by aggregation phenomena, with detrimental effects on the ultimate tensile properties. More relevant improvements can be observed when a fracture mechanics test methodology is adopted for determining the material toughness. K_{IC} and G_{IC} values of pure epoxy and of the nanofilled adhesives are summarized in Fig. 6a,b, respectively. In the case of Cloisite 30B nanocomposites, a maximum K_{IC} value of about 1.4 MPa m$^{1/2}$ (i.e. an 80% increment with respect to the neat resin) can be observed at a filler content of 1 wt%. The fracture toughness improvement is even more enhanced when G_{IC} values are considered. In fact, Epoxy-30B-1 sample shows a G_{IC} of about 1.1 kJ m^{-2}, that is, a value 3.5 times higher than that of pure epoxy resin. Accordingly to quasi-static tensile tests, the subsequent decrease of K_{IC} and G_{IC} values at elevated filler loadings could be probably related to the presence of aggregated clay tactoids. Similar increments of the fracture toughness have been already reported in the scientific literature on epoxy–clay nanocomposites.[22,36] It could be hypothesized that the presence of clay lamellae may render the crack propagation path more tortuous, with a positive contribution on the fracture toughness of the material. This hypothesis is confirmed by ESEM observations of the fracture surfaces of the SENB specimens reported in Fig. 4. It is worthwhile to note that the fracture toughness improvements observed for bulk adhesives samples filled with Cloisite 25A are slightly lower than those detected for 30B filled samples. As an example, K_{IC} and G_{IC} values of Epoxy-25A-1 sample are, respectively, 59% and 128% higher than that of the neat epoxy resin. As previously discussed, XRD tests revealed that a better dispersion of the clay lamellae could be reached by using more hydrophilic clays.

Single-lap bonded joints

Nominal shear strength values determined from quasi-static tensile tests on single-lap joints are reported in Fig. 7. It is evident

(a)

(b)
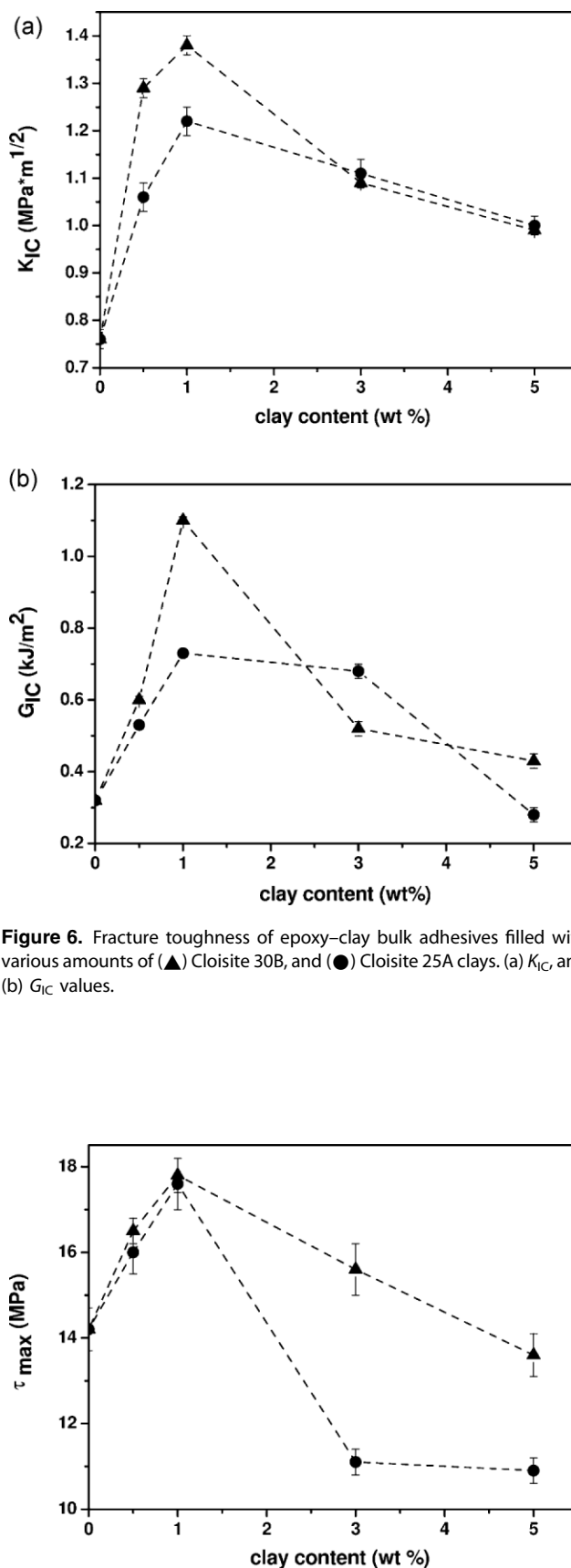
Figure 6. Fracture toughness of epoxy–clay bulk adhesives filled with various amounts of (▲) Cloisite 30B, and (●) Cloisite 25A clays. (a) K_{IC}, and (b) G_{IC} values.

Figure 7. Nominal shear strength of single-lap composite joints prepared with epoxy–clay adhesives filled with various amounts of (▲) Cloisite 30B, and (●) Cloisite 25A clays.

that the introduction of nanoclay in these epoxy adhesive leads to a significant enhancement of the shear resistance of the composite joints. In fact, the maximum shear stress sustained by the Epoxy-30B-1 nanocomposite joint is about 25% higher than that reached using an unfilled epoxy adhesive. At higher filler contents, the shear strength decreases. Even in this case, it could be hypothesized that the presence of clay agglomerates may play a detrimental effect on the mechanical behavior of the joints. It is also possible that the increase of the adhesive viscosity at elevated clay contents produces a non-optimal distribution of the adhesive in the overlapping region. Also the difficulties of the degassing process experienced at elevated filler amounts, due to the high viscosity of the resin, should be taken into account. In the region of elevated filler content, the shear resistance of joints prepared with epoxy containing Cloisite 30B is higher than that of joints based on Cloisite 25A. The observed increase of the shear strength for nanocomposite epoxy joints is in agreement with the conclusions reported by Park and Lee[17] on carbon black reinforced adhesive systems and by Patel et al.[16] on nanomodified acrylic adhesives. Furthermore, the existence of an optimum filler content was reported by Xi et al.[18] on different systems, like graphite nanocomposite adhesives and by Yu et al.[19] on CNTs reinforced epoxy adhesive joints.

For all the tested joints, some adhesive remains on both the substrates after failure, thus evidencing that a cohesive fracture mechanism occurred. Under these fracture conditions, the reinforcing effect experienced in nanocomposite joints could be directly related to the enhancements of the tensile strength and of the fracture toughness observed for the bulk nanofilled adhesives in quasi-static tensile tests. According to the results reported by Mylavarapu and Woldesenbet,[44] it is possible to hypothesize that the nanoclay present in the bondline may act as crack arresting agent thus restricting the initiated micro-length scale cracks from growing into macro-length scale cracks, and hence increasing the shear resistance of the composite joints. In a parallel study on the same epoxy adhesive used in the present work,[11] mechanical tests on single lap aluminium bonded joints indicated that zirconia nanoparticles led to relevant enhancements of the shear strength of the joints. In particular, the shear strength increased by about 60% for an optimal filler content of 1 vol%, and an adhesive failure mechanism was evidenced for all the tested specimens. Concurrently, a significant decrease of the equilibrium contact angle with water was observed for adhesives containing zirconia nanoparticles. It was therefore concluded that the addition of zirconia nanoparticles effectively improved epoxy adhesives, both by increasing their mechanical properties and by enhancing the interfacial wettability with an aluminium substrate. Even if in other papers the positive contribution of the adhesive nanomodification on the shear resistance of the joints was attributed to a better interfacial wettability and chemical compatibility between the adhesive and the substrate,[9,16] in the present case a cohesive fracture mechanism occurred for all the tested samples. Therefore, the improving effect detected for nanocomposite samples could not be ascribed to a change of the failure modes but rather than to a general improvement of the mechanical properties of the bulk adhesives due to resin nanomodification.

CONCLUSIONS

Epoxy-based nanocomposite adhesives were prepared using two different OM clays at various filler concentrations. An intercalated structure was detected from XRD tests, with d-spacing values of the nanoplatelets increasing with the hydrophilicity degree of the OM clay. The optical transparency of the samples was preserved up to a filler content of 3 wt%. The glass transition temperature of Cloisite 30B filled epoxy adhesives increased up to a filler loading of 3 wt% and then decreased, probably because of the contrasting effects of chain blocking and reduction of the cross-linking degree.

Also the mechanical properties of the bulk adhesives presented a trend with a maximum value for a given filler concentration. Remarkable improvements of the elastic modulus, of the tensile strength and of fracture toughness were found for nanofilled samples, especially when more hydrophilic clay were utilized. Finally, noticeable enhancements of the shear strength of single lap composite joints bonded with nanocomposite adhesives at an optimal filler content of 1 wt% were observed.

REFERENCES

[1] D. Dillard, *Improvements in structural adhesive bonding*. Woodhead Publishing Ltd, Cambridge, UK, **2010**.
[2] E. M. Petrie, *Epoxy adhesive formulations*. McGraw-Hill, New York, **2006**.
[3] W. Brockmann, P. L. Geiß, J. Klingen, B. Schröder, *Klebtechnik*. Wiley-WCH, Weinheim, **2005**.
[4] S. Khoee, A. R. Mahdavian, W. Bairamy, M. Ashjari, *J. Colloid Interface Sci.* **2009**, *336*, 872.
[5] J. He, D. Raghavan, D. Hoffman, D. Hunston, *Polymer* **1999**, *40*, 1923.
[6] A. J. Kinloch, *MRS Bull.* **2003**, *28*, 445.
[7] E. N. Gilber, B. S. Hayes, J. C. Seferis, *Polym. Eng. Sci.* **2003**, *43*, 1096.
[8] S. Sprenger, C. Eger, A. J. Kinloch, *Adhesion* **2003**, 20.
[9] S. G. Prolongo, M. R. Gude, J. Sanchez, A. Urena, *J. Adhes.* **2009**, *85*, 180.
[10] K. T. Hsiao, J. Alms, S. G. Advani, *Nanotechnology* **2003**, *14*, 791.
[11] A. Dorigato, A. Pegoretti, F. Bondioli, M. Messori, *Composite Interfaces* **2010**, *17*, 873.
[12] A. Dorigato, A. Pegoretti, *J. Nanoparticle Res.* DOI: 10.1007/s11051-010-0130-0
[13] S. A. Meguid, Y. Sun, *Mater. Des.* **2004**, *25*, 289.
[14] H. S. Hedia, L. Allie, S. Ganguli, H. Aglan, *Eng. Fracture Mech.* **2006**, *73*, 1826.
[15] L. R. Xu, L. Li, C. M. Lukehart, H. J. Kuai, *Nanosci. Nanotechnol.* **2007**, *7*, 2546.
[16] S. Patel, A. Bandyopadhyay, A. Ganguly, A. K. Bhowmick, *J. Adhes. Sci. Technol.* **2006**, *20*, 371.
[17] S. W. Park, D. G. Lee, *J. Adhes. Sci. Technol.* **2009**, *23*, 619.
[18] X. Xi, C. Yu, W. Lin, *J. Adhes. Sci. Technol.* **2009**, *23*, 1939.
[19] S. Yu, M. N. Tong, G. Critchlow, *J. Appl. Polym. Sci.* **2009**, *111*, 2957.
[20] M. Preghenella, A. Pegoretti, C. Migliaresi, *Polymer* **2005**, *46*, 12065.
[21] G. Ragosta, M. Abbate, P. Musto, G. Scarinzi, L. Mascia, *Polymer* **2005**, *46*, 10506.
[22] Q. M. Jia, M. Zheng, C. Z. Xu, H. X. Chen, *Polym. Adv. Technol.* **2006**, *17*, 168.
[23] F. Bondioli, V. Cannillo, E. Fabbri, M. Messori, *Polimer* **2006**, *51*, 794.
[24] R. Medina, F. Haupert, A. K. Schlarb, *J. Mater. Sci.* **2008**, *43*, 3245.
[25] B. Akbari, R. Bagheri, *Eur. Polym. J.* **2007**, *43*, 782.
[26] M. Alexandre, P. Dubois, *Mater. Sci. Eng.* **2000**, *28*, 1.
[27] C. Basara, U. Yilmazer, G. Bayram, *J. Appl. Polym. Sci.* **2005**, *98*, 1081.
[28] D. Dean, R. Walker, M. Theodore, E. Hampton, E. Nyairo, *Polymer* **2005**, *46*, 3014.
[29] I. Isik, U. Yilmazer, G. Bayram, *Polymer* **2003**, *44*, 6371.

[30] T. J. Pinnavaia, G. W. Beall, *Polymer clay nanocomposites*. John Wiley & Sons, New York, **2000**.

[31] A. Yasmin, J. L. Abot, I. M. Daniel, *Scr Med* **2003**, *49*, 81.

[32] X. Kornmann, H. Lindberg, L. A. Berglund, *Polymer* **2001**, *42*, 1303.

[33] S. C. Tjong, *Mater. Sci. Eng. R Rep.* **2006**, *53*, 73.

[34] I. Jan, T. Lee, K. Chiu, J. Lin, *Ind. Eng. Chem. Res.* **2005**, *44*, 2086.

[35] A. Pegoretti, A. Dorigato, M. Brugnara, A. Penati, *Eur. Polym. J.* **2008**, *44*, 1662.

[36] W. Liu, S. V. Hoa, M. Pugh, *Composites Sci. Technol.* **2005**, *65*, 2364.

[37] S. C. Zunjarrao, R. Sriraman, R. P. Singh, *J. Mater. Sci.* **2006**, *41*, 2219.

[38] A. Pegoretti, M. L. Accorsi, A. T. DiBenedetto, *J. Mater. Sci.* **1996**, *31*, 6145.

[39] A. Dorigato, S. Morandi, A. Pegoretti, Morphological and thermo-mechanical characterization of epoxy-clay nanocomposites. In: *ETDCM9 - 9th seminar on experimental techniques and design in composite materials*. Vicenza University Press, Vicenza, Italy, **2009**.

[40] V. Nigam, D. K. Setua, G. N. Mathur, K. K. Kar, *J. Appl. Polym. Sci.* **2004**, *93*, 2201.

[41] Y. Ke, J. Lu, X. Yi, J. Zhao, Z. Qi, *J. Appl. Polym. Sci.* **2000**, *78*, 808.

[42] S. Benfarhi, C. Decker, L. Keller, K. Zahouily, *Eur. Polym. J.* **2004**, *40*, 493.

[43] T. P. Mohan, M. R. Kumar, R. Velmurugan, *J. Mater. Sci.* **2006**, *41*, 2929.

[44] P. Mylavarapu, E. Woldesenbet, *J. Adhes. Sci. Technol.* **2010**, *24*, 389.

Copyright © 2011 John Wiley & Sons, Ltd.